

Sedimentation measurements with the analytical ultracentrifuge with absorption optics: influence of Mie scattering and absorption of the particles

M. D. Lechner · Helmut Cölfen · Vikas Mittal ·
Antje Völkel · Wendel Wohlleben

Abstract Analytical ultracentrifugation is one of the most powerful methods for the characterization of nanoparticles since the days of its invention due to its high resolution and statistical significance. Latexes with different sizes and their mixtures have been measured by sedimentation with the analytical ultracentrifuge (AUC) OPTIMA XL-I (Beckman Coulter, Palo Alto, CA, USA) with interference optics at $\lambda_0=675$ nm and absorption optics at $\lambda_0=546$ and 263 nm. Additionally, a blue pigment with high absorption characteristic at visible light has been investigated. A large influence of Mie scattering and Mie absorption on the particle size distribution with respect to absorption optics and samples with moderate or broad size distribution is observed. Therefore, the consideration of the Mie scattering effect is compulsory for most AUC measurements of nanoparticles with absorption optics.

Keyword Analytical ultracentrifugation · Particle size distribution · Mie scattering · Absorption · Extinction · Mie correction

M. D. Lechner (✉)
Physical Chemistry, University of Osnabrueck,
Barbarastrasse 7,
49069 Osnabrueck, Germany
e-mail: lechner@uni-osnabrueck.de

H. Cölfen · A. Völkel
Physical Chemistry, University of Konstanz,
Universitätsstrasse 10,
78457 Konstanz, Germany

V. Mittal · W. Wohlleben
Polymer Physics Research, BASF SE,
67056 Ludwigshafen, Germany

Introduction

Sedimentation velocity measurements with the analytical ultracentrifuge (AUC) OPTIMA XL-I with absorption optics yield not only the size but also the complete size distribution of the dissolved or dispersed particles [1, 2]. The problem which arises from the influence of Mie scattering on the signal of the detector for the determination of the sample concentration has been solved by different authors [1–4]. Nevertheless Mie correction procedures have not been implemented up to now into the available software for the OPTIMA XL-I (UltraScan, SedFit, etc.). While the influence of Mie scattering is not significant for dissolved macromolecules, it is certainly significant for nanoparticles due to their bigger size. Since the investigation of nanoparticles and aggregates with ultracentrifugation techniques becomes increasingly important [5], it is important to investigate the relevance of Mie scattering for the evaluation of experiments using the UV–Vis absorption optics. It will be shown in this contribution that the differences of non-Mie-corrected and Mie-corrected size distributions are remarkable especially for particles with diameters (d) of >15 nm.

Additionally, the influence of the detector signal of absorbing and/or colored particles (i.e., pigments and polymers) which absorb at the same wavelength as the wavelength of the light source has been examined. To the best of our knowledge, this problem was not addressed up to now for the AUC.

Theoretical considerations

Particles, detected with absorption optics, follow Lambert–Beer’s law [5]:

$$\ln(I_0/I) = \varepsilon C l = a l \quad (1)$$

with I_0/I =ratio of the intensities of the solvent and the solution, ε =extinction coefficient, α =extinction module, C =mass concentration of the dissolved or dispersed particles (mass per volume), and l =path length.

For spherical particles, the diameter (size) d and the size distribution $w(d)$ may be calculated according to Stokes' law [4]:

$$d^2 = 18 \eta_0 S / (\rho - \rho_0) \quad ; \quad S = (1/\omega^2)(d \ln r/dt) \quad (2)$$

and the concentration $C(r)$ at the distance from the center of rotation r ; with ρ =density of the particle, ρ_0 =density of the solvent, η_0 =viscosity of the solvent, S =sedimentation coefficient, $\omega=2\pi N$ =angular velocity of the rotor, and N =rotor speed.

Generally speaking, the absorption optics of an AUC measures not only the scattered intensity of a particle but also the absorbed intensity of the particle. The sum of the scattered and the absorbed intensity is called extinction [6]. Strictly speaking, the absorption optics in an AUC measures the extinction of the particles. The extinction may be reduced to only scattering if the particles do not absorb at the considered wavelength. In addition, strong refractive index gradients can bend the light out of the optical path resulting in an artificial light absorption, which is called a Schlieren effect [7], but this does not need to be considered for typical experiments.

The extinction coefficient ε may be calculated by Mie's scattering theory [8]. Starting with Maxwell's equations, the extinction efficiency Q_{ext} as a function of the size parameter $\pi d/\lambda$ (d =diameter, $\lambda=\lambda_0/n_0$ =wavelength), the density of the particle ρ , and the refractive indices of the solvent n_0 and the particle n_1 have been developed. In the case that the incident light is not only scattered but also absorbed by the particle, the complex refractive index of the particle

$$N_1 = n_1 + i k_1 \text{ with } i = (-1)^{1/2} \quad (3)$$

(k_1 is the imaginary part of the refractive index) instead of only n_1 has to be applied. Mie calculated Q_{ext} for homogeneous, isotropic spheres [8]. Different authors have calculated Q_{ext} for inhomogeneous spheres with a refractive index gradient, coated spheres, ellipsoids, and cylinders [6].

The relation of the extinction efficiency Q_{ext} and the extinction coefficient ε is given by [6]:

$$\varepsilon = 3 Q_{\text{ext}} / (2 d \rho); \text{ (sphere with diameter } d) \quad (4)$$

$$\varepsilon = \pi Q_{\text{ext}} / (d \rho); \text{ (cylinder with diameter } d \text{ and infinite length)} \quad (5)$$

Figure 1 demonstrates the extinction coefficient ε (sometimes called specific turbidity $\varepsilon=\pi/C$) as a function of the reduced size parameter $\pi d/\lambda$ for different ratios n_1/n_0

for spheres. The ε values were calculated according to Mie's theory [6, 8] and according to Eq. 4, with $\rho=1 \text{ g/cm}^3$. For densities of the particles which differ from unity, one has to divide the ε values by ρ . The lower diameter scale refers to a wavelength $\lambda_0=546.1 \text{ nm}$ and a refractive index of the solvent of $n_0=1.333$. The rippling of some curves is due to oscillations of the Bessel functions included in Mie's equations. The figures show that Mie's theory includes the Rayleigh scattering of small molecules with diameters down to 1 nm. As has been shown by Dezelic and Kratochvil, the theories of Rayleigh and Mie are nearly identical with respect to the extinction coefficient in the range $0 < \pi d/\lambda < 0.3$ [9]. Figure 1 indicates the angle independent Rayleigh scattering ($d < \lambda/20$), the angle-dependent Rayleigh scattering ($\lambda > d > \lambda/20$), and the Mie scattering ($d > \lambda$) [10, 11].

Figure 2 shows the extinction coefficient ε for cylinders with infinite length and diameter d . The calculations are done in the same way as for spheres and coated spheres. The extinction efficiency Q_{ext} for cylinders is given in the literature [6]. As the calculation is done for cylinders with infinite length, the experimental results fit best the theoretical values for sufficiently large l/d values (l is the length of the cylinder). Figure 2 demonstrates remarkable differences between spheres and cylinders with respect to the extinction coefficient.

Figure 3 compares the extinction coefficient ε of coated spheres with different values for n_1/n_0 for $n_2/n_0=1.10$ and $d_1=(d-5) \text{ nm}$; one curve has been calculated with $k_1=0.02$ (k_1 is the imaginary part of the refractive index). Dependent on the different diameters and the refractive indices, the differences with respect to uncoated spheres are significant. Coated spheres with constant thickness of the coat are typical for grafted polymer particles and liposomes.

The calculation of ε in conjunction with Lambert-Beer's law (Eq. 1) enables the determination of the concentration of the particles C if the optical density $\ln(I_0/I)$ and the thickness of the solution in a cuvette could be measured. Fractionation of the particles by applying a gravitational or centrifugal field allows the determination of the particle size distribution.

In the case of absorbing particles (i.e., pigments or polymers which would be detected at lower wavelength), the imaginary part of the refractive index could be measured in the following way. As has been already pointed out, a beam of light passing a medium is both attenuated by absorption and by scattering. The extinction efficiency Q_{ext} is therefore the sum of the absorption efficiency Q_{abs} and the scattering efficiency Q_{sca} [6, 12]:

$$Q_{\text{ext}} = Q_{\text{abs}} + Q_{\text{sca}} \quad (6)$$

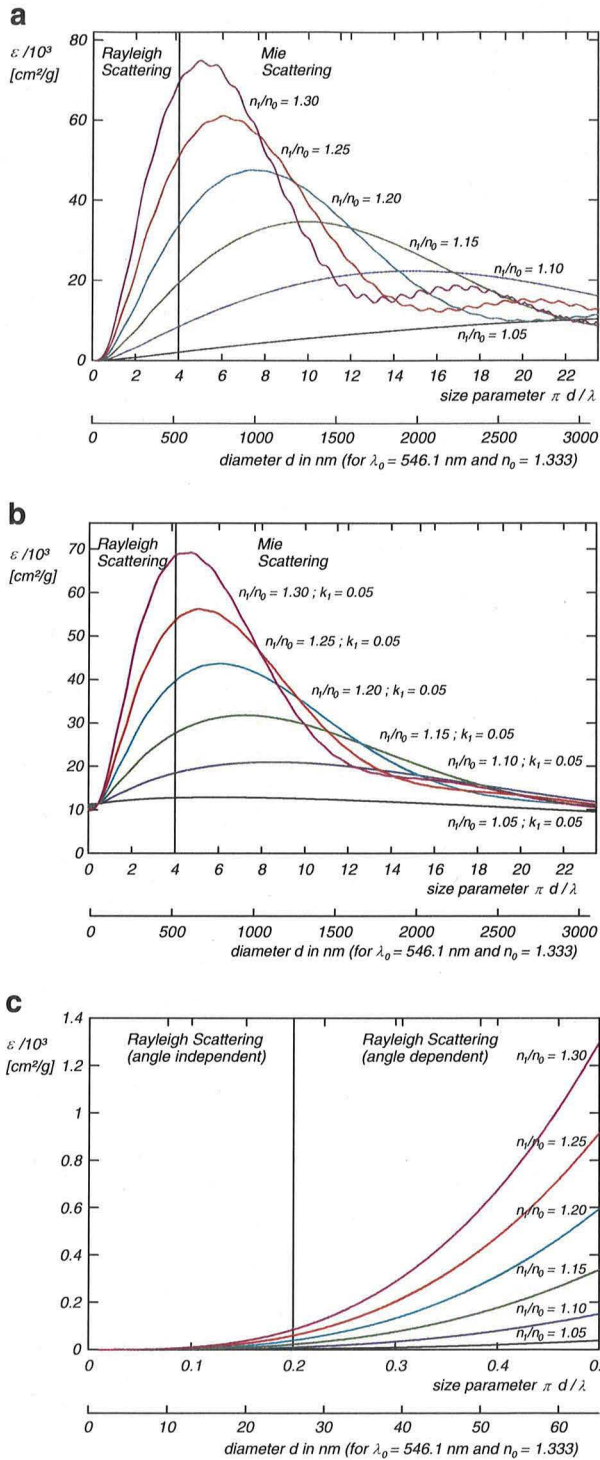


Fig. 1 a-c Particle scattering: extinction coefficient ϵ for spheres with $k_1=0$ (a, c) and $k_1=0.05$ (b) as a function of the size parameter $\pi d/\lambda$ for different relations of the refractive indices n_1/n_0 in the regions $0 < \pi d/\lambda < 15$ (a, b) and $0 < \pi d/\lambda < 0.5$ (c); the lower diameter axis refers to $\lambda_0=546.1$ nm and $n_0=1.333$

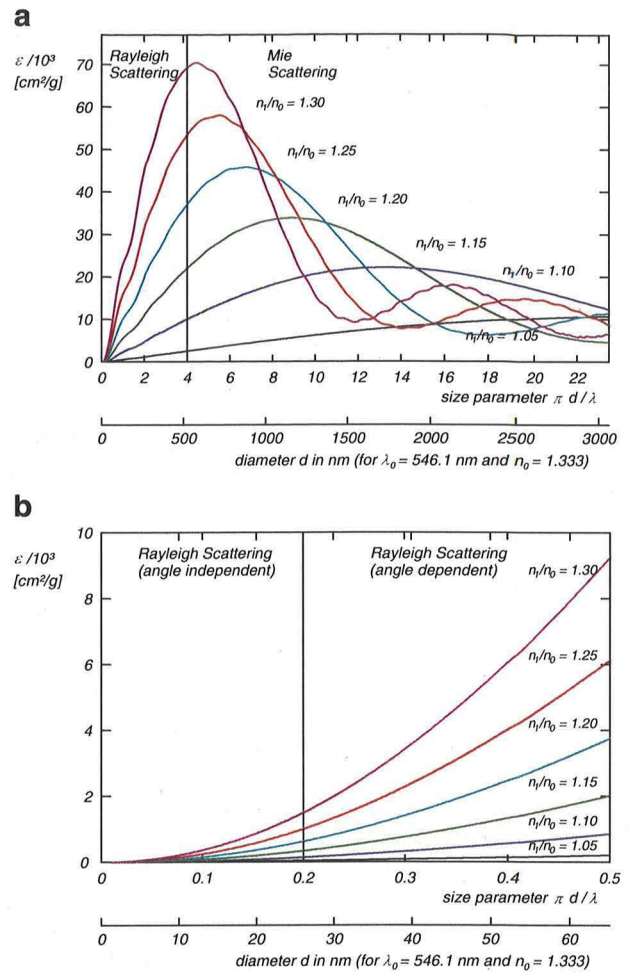


Fig. 2 a, b Particle scattering: extinction coefficient ϵ for cylinders with $k_1=0$ as a function of the size parameter $\pi d/\lambda$ for different relations of the refractive indices n_1/n_0 in the regions $0 < \pi d/\lambda < 15$ (a) and $0 < \pi d/\lambda < 0.5$ (b); the lower diameter axis refers to $\lambda_0=546.1$ nm and $n_0=1.333$

As Q_{ext} is, according to Eqs. 1, 4, and 5, proportional to ϵ and α , it holds [6]:

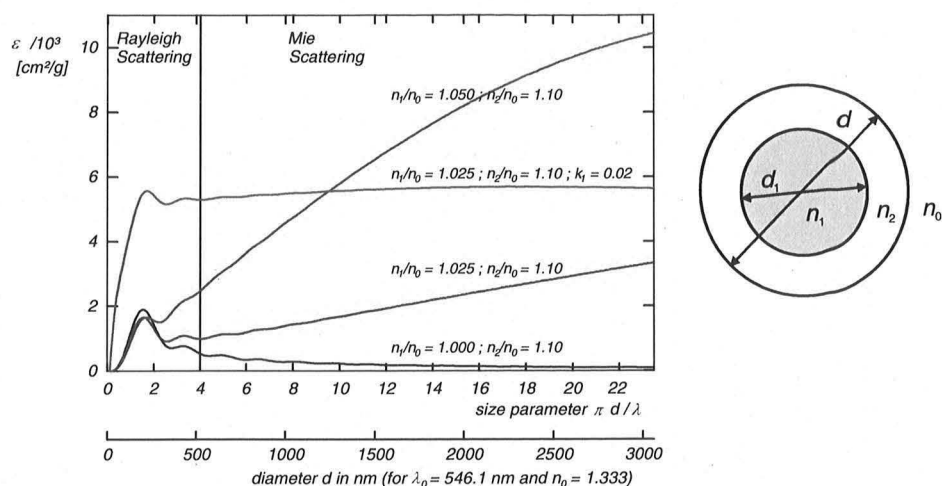
$$\alpha = \alpha_{\text{ext}} = \alpha_{\text{abs}} + \alpha_{\text{sca}} \quad (7)$$

The relationship between α_{abs} and the imaginary part of the refractive index k_1 is given by [12]:

$$k_1 = \alpha_{\text{abs}} \cdot \lambda_0 / (4\pi) \quad (8)$$

with λ_0 as the wavelength in vacuo. As the calculation of the extinction coefficient ϵ with Mie's theory needs k_1 , Eqs. 1 and 8 are the basis for its determination. Unfortunately, a spectrometer measures both absorption and scattering and therefore α_{ext} . It would be therefore necessary to determine α_{sca} to obtain α_{abs} according to Eq. 7.

Fig. 3 Particle scattering: extinction coefficient ε with $k_1=0$ and $k_1=0.02$ for coated spheres as a function of the size parameter $\pi d/\lambda$ for different relations of the refractive indices n_1/n_0 in the region $0 < \pi d/\lambda < 15$ for $n_2/n_0=1.10$ and $d_1=(d-5)$ nm; the lower diameter axis refers to $\lambda_0=546.1$ nm and $n_0=1.333$



Although absorption and scattering occur principally simultaneously, there are a couple of examples where either absorption or scattering dominates the other effect. For example, visible light passing a synthetic polymer solution or dispersion is attenuated almost entirely by scattering (in this case, $k_1=0$), whereas light passing through a pigment solution might be primarily attenuated by absorption (in this case, $\alpha_{\text{abs}}=\alpha_{\text{ext}}$), and k_1 may be obtained by spectrometric measurements and Eq. 8.

The most complicated situation—absorption and scattering of the dissolved or dispersed particles—may be solved with spectrometric and light scattering measurements with the help of Eqs. 7 and 8. Spectrometric measurements exhibit α_{ext} whereas light scattering measurements exhibit α_{sca} ; integration of the scattering intensities $R(\theta)$ from 0 to 180° yields

$$\alpha_{\text{sca}} = \int_0^{180} R(\theta) d\theta \quad (9)$$

For sufficiently small molecules ($d < \lambda/20$) and unpolarized light, it holds [12]:

$$\alpha_{\text{sca}} = (16\pi/3)R(90) \quad (10)$$

The AUC OPTIMA XL-I has a variable slit moving during distinct times from the meniscus to the bottom. A lamp illuminating the slit together with a light detector measures the intensity $I(r)$ as a function of the distance from the center of rotation r . Following Eq. 1, the ratio of the extinction module at the distance r , $\alpha(r)=\varepsilon(r)C$ and the initial extinction module $\alpha_{\text{in}}=\varepsilon_{\text{in}}C$ could be determined via the experimentally accessible intensities of the solution and the solvent:

$$\alpha(r)/\alpha_{\text{in}} = \{\ln[I(r)/I_0]\}/\{\ln[I_{\text{in}}/I_0]\} \quad (11)$$

with $I(r)$, I_{in} , and I_0 =intensities of the solution at the distance r , initial intensity, and intensity of the solvent,

respectively. In the case that all dissolved or dispersed particles have identical extinction coefficients $\varepsilon_i=\varepsilon$, the relative concentration of the particles and the integral size distribution function could easily be determined:

$$\alpha(r)/\alpha_{\text{in}} = C(r)/C_{\text{in}} = W(d) \quad (12)$$

Using an analytical ultracentrifuge, particles with different diameters (sizes) d could be fractionated according to their diameter using Stokes' well-known law [4]:

$$d_i^2 = 18\eta_0 S_i / [\rho - \rho_0]; S_i = [\ln(r/r_h)] / \int \omega^2 dt \quad (13)$$

with d_i =diameter (size) of the species i , η_0 =viscosity of the solvent, S_i =sedimentation coefficient of the species i , ρ =density of the particle, ρ_0 =density of the solvent, r =distance from center of rotation (radial position) in the ultracentrifuge cell, $r_h=r_m$ =radius position of the meniscus in the cell in the case of sedimentation of the particles, $r_h=r_b$ =radius position of the bottom in the cell in the case of flotation of the particles, and ω =angular velocity of the rotor.

For sector-shaped cells, the dilution rule has to be applied:

$$C(r)/C_{\text{in}} = (r_h/r)^2 \quad (14)$$

In the case of different particle sizes, one has to apply for each species a different extinction coefficient $\varepsilon_i=(\alpha/C)_i$ according to Eqs.4 and 5:

$$\alpha(r)/\alpha_{\text{in}} = \sum_{i=1}^N \alpha_i(r)/\alpha_{\text{in}} = (1/\varepsilon_{\text{in}}) \sum_{i=1}^N \varepsilon_i C_i(r)/C_{\text{in}} \quad (15)$$

with $i=1, 2, \dots, N$ being the species number.

Using an AUC OPTIMA XL-I with absorption optics, the evaluation procedure is as follows: Considering the measured absorption (better: extinction!) $I(r)/I_0$ curve as a

superposition of $N I(r)/I_0$ curves for monodisperse particles, the evaluation starts with determining the first derivative of the $I(r)/I_0$ curve. The derivative may be calculated using a regression spline function in order to get rid of the noise from window and other defects; this procedure is implemented in the program VelXLAI. In this way, one gets $I(r)/I_0$ for each species with a distinct diameter d_i which is calculated according to Eq. 13. The appropriate concentration $C_i(r)$ could be determined according to Eqs. 1, 4, 5, and 14; the differential size distribution function $w(d)$ would be:

$$w(d) = C_i(r)/C_{in} \tag{16}$$

Integration yields the cumulative size distribution function $W(d)$:

$$W(d) = \int w(d)dd = \int g(S)dS \tag{17}$$

The calculation of the extinction coefficient ε with Mie's theory needs the refractive index of the dissolved or dispersed particle n_1 ; in case that this quantity could not directly be measured, it could be calculated with the help of the refractive index increment of the dispersion or solution dn/dC . The combination of Gladstone–Dale's specific

refraction equation $R_{GD}=(n-1)/\rho$ and the mixture rule for the specific refraction $R=w_0 R_0+w_1 R_1$ yields [13]:

$$n_1 = (dn/dC)\rho_1 + n_0 \tag{18}$$

dn/dC can be easily measured with a differential refractometer.

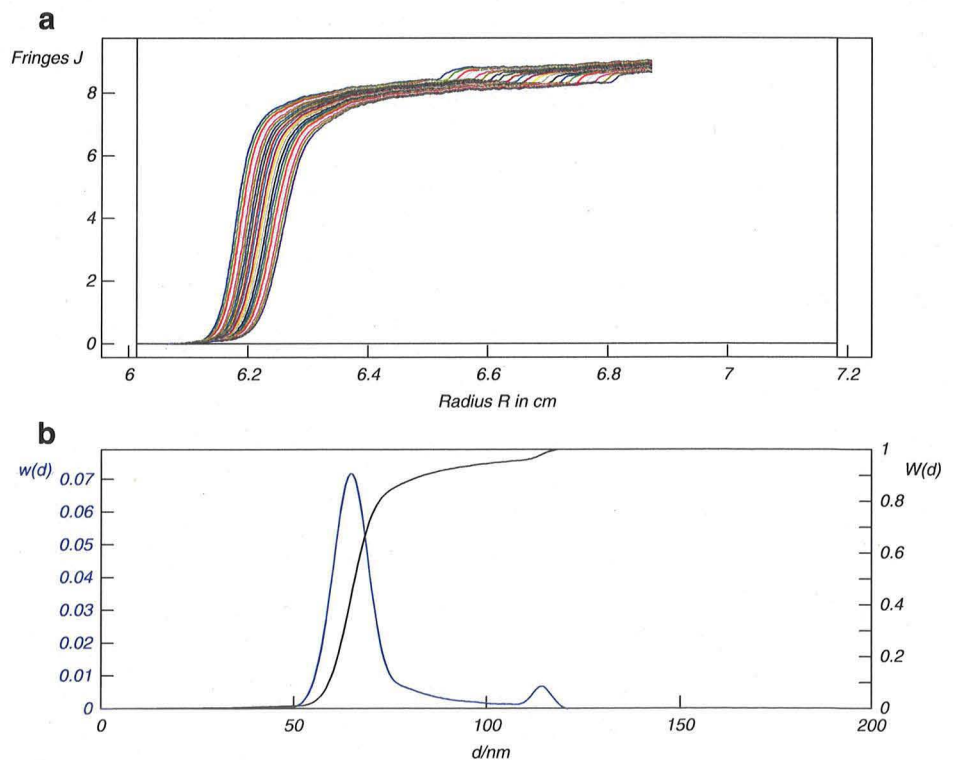
Experimental materials and methods

Materials

Latex B66 and Latex B79 are polystyrene polymers and were prepared by standard emulsion polymerization [14]. The diameters are given as 66 ± 2 nm (B66) and 119 ± 2 nm (B79). Latexmix B66/B79 was a mixture of both latexes with a mass ratio $m(B66)/m(B79)=9:1$. The latexes and their mixtures were dispersed in water. The density of the latexes was $\rho_1=1.054$ g/cm³. The refractive index increment was measured with a commercially available differential refractometer and was 0.25 cm³/g; Equation 18 exhibits (with $n_0=1.333$) $n_1=1.59$ for $\lambda_0=675$ nm. The refractive index of the latex n_1 coincides with values in the literature [15, 16].

Latex Duke3060A and Latex Duke3100A are pure polystyrene spheres which are commercially available (Duke Scientific, Palo Alto, CA, USA). The diameters are

Fig. 4 OPTIMA XL-I, interference optics: size distribution of a Latexmix B66/B79 ($d=66$ and 119 nm; mass ratio, 9:1) in water; $C=2.2$ g/L, $\rho=1.054$ g/cm³, $\rho_0=0.997$ g/cm³, $dn/dC=0.25$ cm³/g, $\lambda_0=675$ nm, $N=10,000$ min⁻¹; **a** Interference scan, **b** evaluation, size distribution



given as 59 ± 2 nm (Duke3060A) and 102 ± 3 nm (Duke3100A). Latexmix Duke3060A/Duke3100A was a mixture of both latexes with a mass ratio $m(\text{Duke3060A})/m(\text{Duke3100A})=74:26$. The density of the latexes was $\rho_1=1.054$ g/cm³. The refractive index increment was measured with a commercially available differential refractometer and was 0.23 cm³/g; Equation 18 exhibits (with $n_0=1.334$) $n_1=1.58$ for $\lambda_0=546$ nm and (with $n_0=1.370$) $n_1=1.61$ for $\lambda_0=263$ nm. These data agree with data given in the literature [15, 16]

The blue pigment was produced by BASF SE by formulating the absorbing core with polymers; it was dispersed in water. The density of the solute was 1.39 g/cm³, the real part of the refractive index was 1.30, and the

imaginary part was 0.153, as determined by spectroscopy on an unfractionated sample.

Methods

For the experiments on the latexes, a commercially available Beckman Analytical Ultracentrifuge OPTIMA XL-I with absorption and interference optics was used with the following physical parameters: cell path length, 1.2 cm; center piece, Ti; rotor speed, 10,000 min⁻¹ (B66, B79) and 7,500 min⁻¹ (Duke3060A, Duke 3100A); temperature, 25 °C; and wavelength, 675 nm (interference optics), 360 nm (absorption optics, B66, B79), 263 nm, and 546 nm (absorption optics, Duke3060A and Duke 3100A).

Fig. 5 OPTIMA XL-I, absorption optics: size distribution of a Latexmix B66/B79 ($d=66$ and 119 nm; mass ratio, 9:1) in water; $C=0.55$ g/L, $\rho=1.054$ g/cm³, $\rho_0=0.997$ g/cm³, $\lambda_0=360$ nm, $N=10,000$ min⁻¹; **a** Absorption scan, **b** evaluation without Mie correction, **c** evaluation with Mie correction, $n_0=1.333$, $n_1=1.59$, $k_1=0$

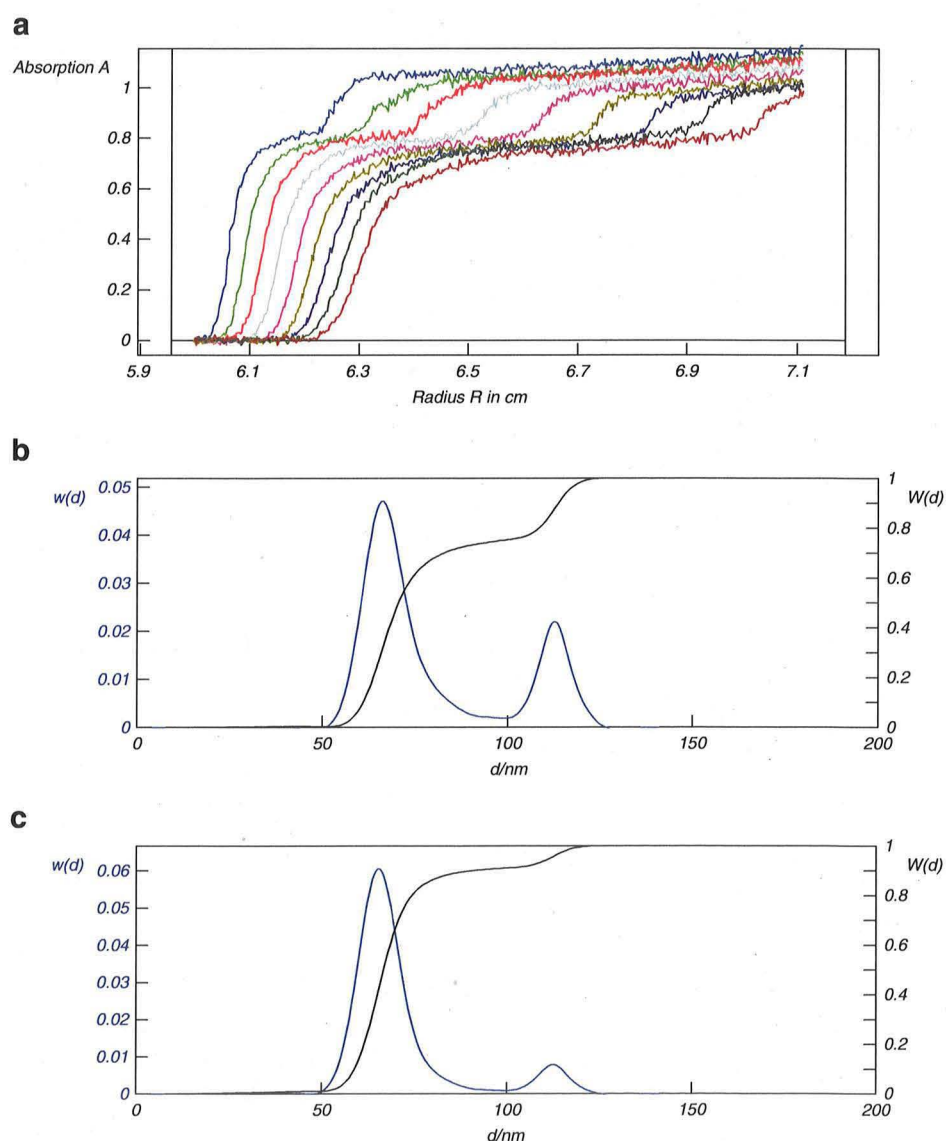


Table 1 Diameters and mass ratios of latexes and latex mixtures B66, B79, Duke3060A, and Duke 3100A measured using (AUC) OPTIMA XL-I with interference optics and absorption optics

Sample	Latex B66	Latex B79	Latex B66/B79	Latex Duke3060A	Latex Duke3100A	Latex Duke3060A/Duke3100A
Factory (d/nm)	66±2	119±2		59±2	102±3	
Loading ratio			90:10			74:26
Interference optics (d/nm)	65.5±2	117±2		60.5±2	100.5±2	
Absorption optics (d/nm)	65±2	112±2		60.5±2	99.5±2	
Ratio interference optics 675 nm			91:9			75:25
Ratio absorption optics, no Mie 546 nm			72:28			48:52
Ratio absorption optics, Mie 546 nm			91:9			76:24
Ratio absorption optics, no Mie 263 nm						50:50
Ratio absorption optics, Mie 263 nm						71:29

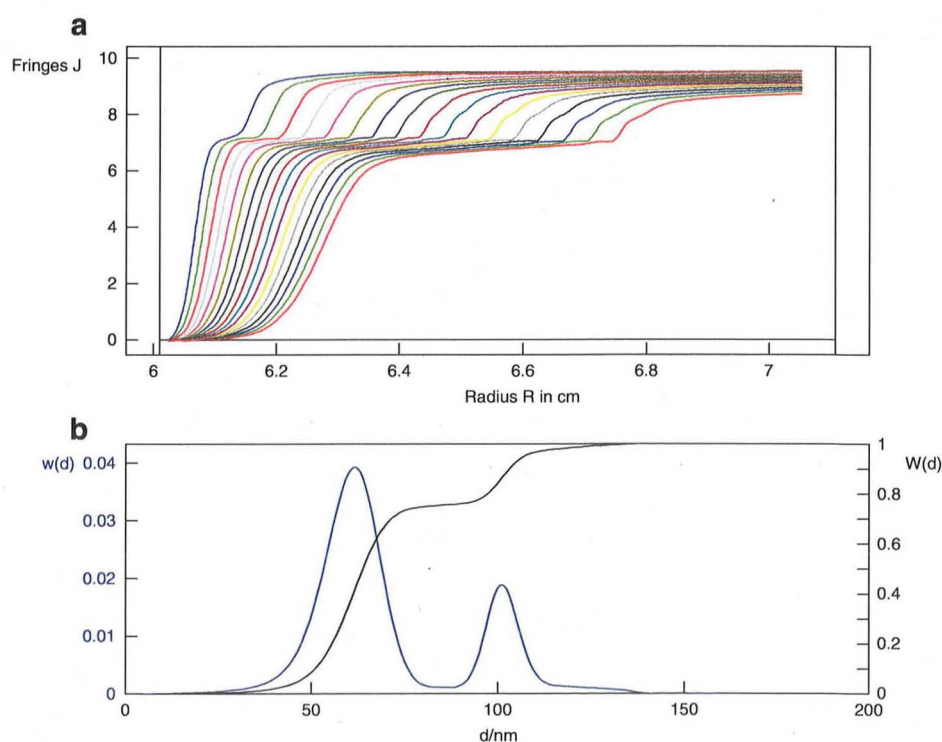
Ratio mass ratio of the two samples

The absorption optics was adjusted to step: 0.003 cm; no. of replicates, 1; and time of scans, any 4–5 min. Both interference and absorption measurements were made in the same cell and the same run. The measurements with the blue pigment were done with a Beckman OPTIMA XL with homemade absorption optics and with the following physical parameters: cell path length, 1.2 cm; center piece, Ti; rotor speed, 0–40,000 min^{-1} with exponential increase of the rotor speed; temperature, 25 °C; and wavelength, 546 nm.

The evaluation was done using the program VelXLAI [17]; this program evaluates both interference and absorption optics measurements and includes a Mie correction with respect to the absorption optics. The program VelXLAI is available, in principle, from one of us (M.D.L.) upon execution of a license agreement with BASF SE, Ludwigshafen.

Among a couple of methods for the determination of the size distribution, a method termed as Gosting Fujita Lechner [18–20] method, which is free from any model assumptions, has been used. The time-dependent (and in the case of

Fig. 6 OPTIMA XL-I, interference optics: size distribution of a Latexmix Duke60/Duke100 ($d=60$ and 100 nm; mass ratio, 74:26) in water; $C=2.54$ g/L, $\rho=1.054$ g/cm³, $\rho_0=0.997$ g/cm³, $dn/dC=0.23$ cm³/g, $\lambda_0=675$ nm, $N=7,500$ min^{-1} ; **a** Interference scan, **b** evaluation, size distribution



nonspherical particles, concentration-dependent) sedimentation coefficient and its distribution could be determined according to

$$S(C, t) = (dr/dt)/(\omega^2 r) = (1/\omega^2) d \ln r / dt \\ = \ln(r/r_m) / \left(\int \omega^2 dt \right) \quad (19)$$

$$g(S, C, t) = (1/C_0) [dC(r, t)/dr] (r/r_m)^2 r \int \omega^2 dt \quad (20)$$

C_0 is the loading concentration of the particles and $C(r, t)$, the concentration at distance r from center of rotation and running time t . Keeping in mind that the sedimentation is proportional to the running time t and the diffusion proportional to the square root of the running time $t^{1/2}$, the extrapolation of $g(S, C,$

$t)$ to $1/t \rightarrow 0$ gives directly and model free $g(S, C)$ [20]. In the case of spherical latexes and pigments, it holds $g(S, C) = g(S)$.

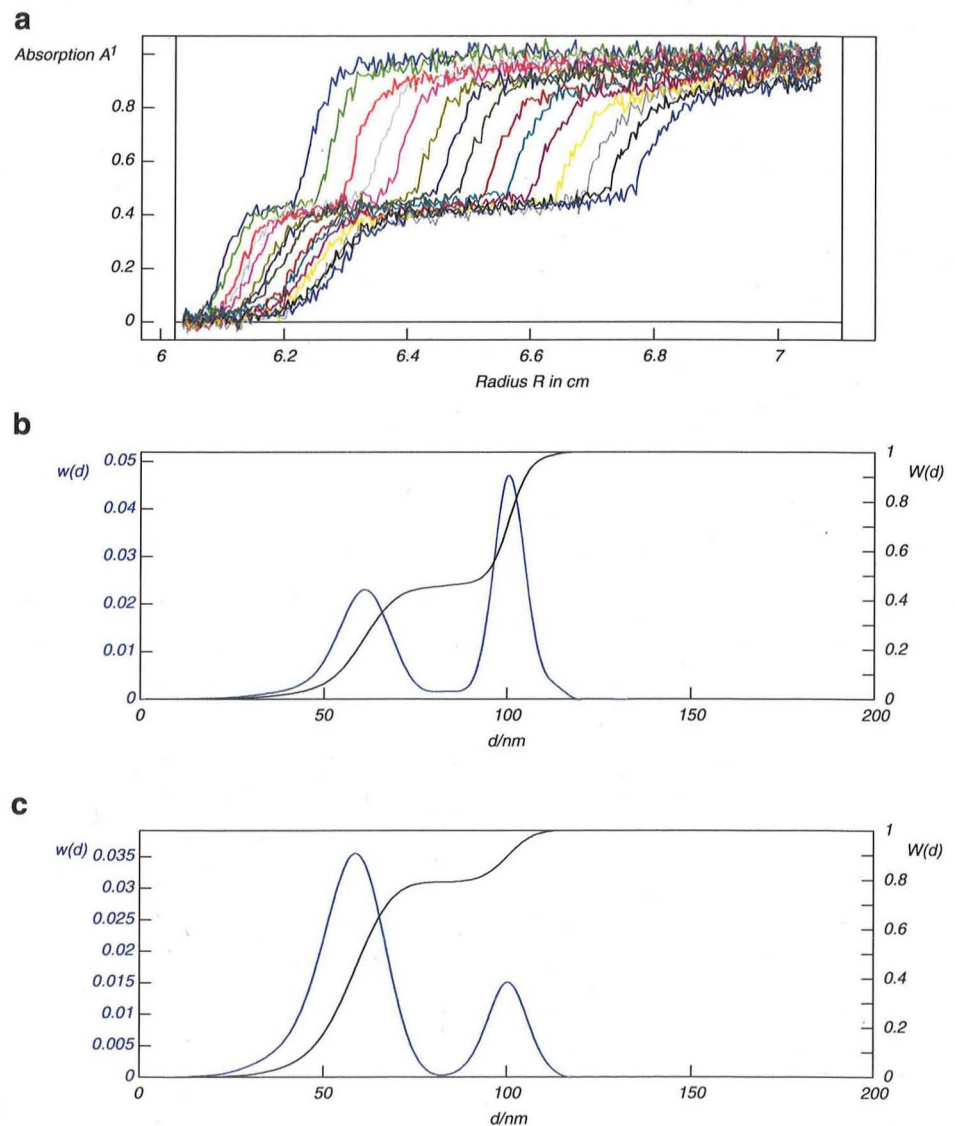
The $w(d)$ size distributions were calculated from 20 scans; the very first (restricted sedimentation near the meniscus) and the very last ("disappearing" of material in the bottom of the cell) scans of the run have been omitted.

Results

Validation

Measurements and evaluations with interference optics with respect to the Latexmix B66/B79 are shown in Fig. 4. Interference optics measurements exhibit no Mie effect; therefore, the measurements yield directly the size distribu-

Fig. 7 OPTIMA XL-I, absorption optics: size distribution of a Latexmix Duke60/ Duke100 ($d=60$ and 100 nm; mass ratio, 74:26) in water; $C=2.54$ g/L, $\rho=1.054$ g/cm³, $\rho_0=0.997$ g/cm³, $\lambda_0=546$ nm; $N=7,500$ min⁻¹; **a** Absorption scan, **b** evaluation without Mie correction, **c** evaluation with Mie correction, $n_0=1.333$, $n_1=1.59$, $k_1=0$



tion. The experimental values agree well with the given values: $d(\text{B66})=65.5\pm 2$ nm; $d(\text{B79})=117\pm 2$ nm; and $m(\text{B66})/m(\text{B79})=91:9$. The diameters are derived from the peak maxima positions in the figures, and the uncertainty for the measured diameters is the variability among replicate measurements of the same sample.

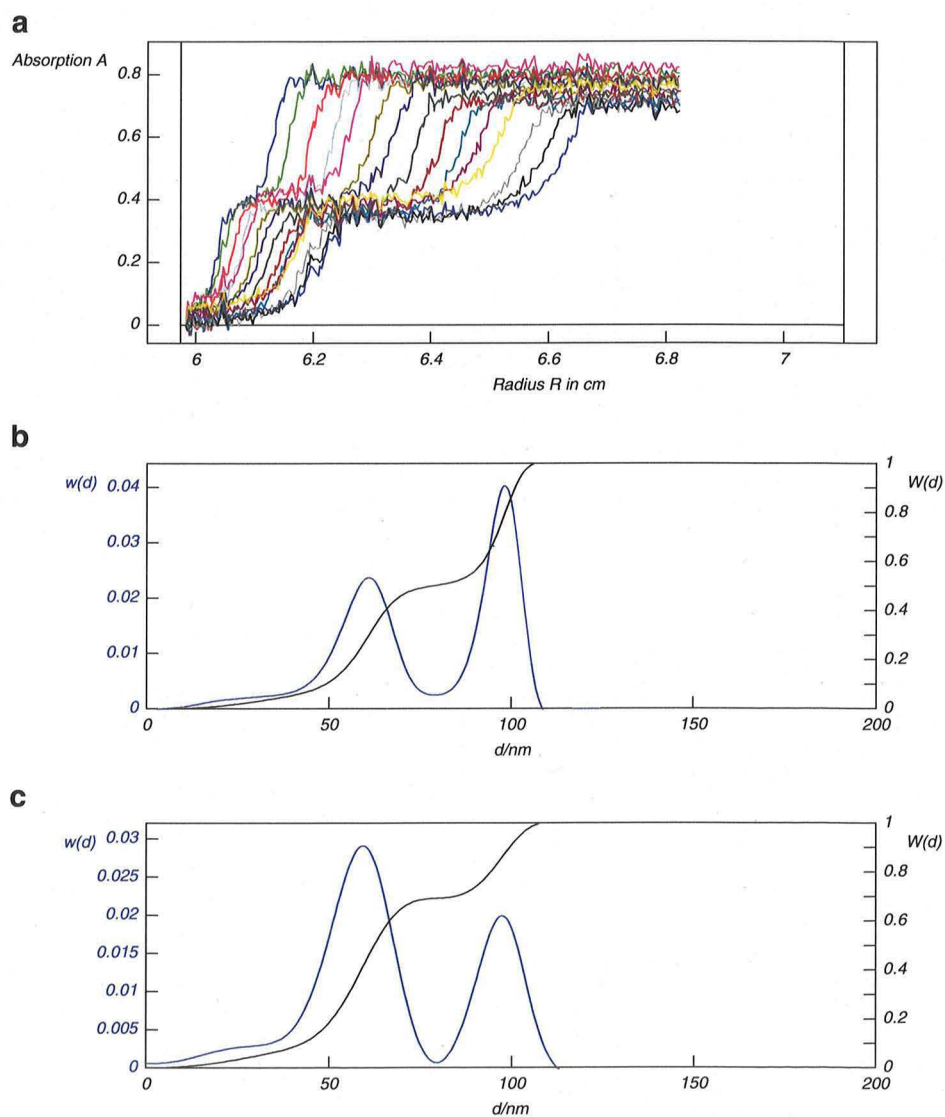
Application

Measurements and evaluations with absorption optics in comparison with interference optics with respect to the Latexmix B66/B79 are shown in Figs. 4 and 5. The results are:

NotMiecorrected : $d(\text{B66}) = 65 \pm 2$ nm; $d(\text{B79}) = 112 \pm 2$ nm; $m(\text{B66}) / m(\text{B79}) = 72 : 28$

Miecorrected : $d(\text{B66}) = 65 \pm 2$ nm; $d(\text{B79}) = 112 \pm 2$ nm; $m(\text{B66}) / m(\text{B79}) = 91 : 9$

Fig. 8 OPTIMA XL-I, absorption optics: size distribution of a Latexmix Duke60/Duke100 ($d=60$ and 100 nm; mass ratio, 74:26) in water; $C=2.54$ g/L, $\rho=1.054$ g/cm³, $\rho_0=0.997$ g/cm³, $\lambda_0=263$ nm; $N=7,500$ min⁻¹; **a** Absorption scan, **b** evaluation without Mie correction, **c** evaluation with Mie correction, $n_0=1.370$, $n_1=1.61$, $k_1=0.005$



The results are summarized in Table 1. Only the Mie-corrected experimental values of the ratio $m(\text{B66})/m(\text{B79})$ agree well with the given values; the differences between the not Mie corrected and the given values of the mass ratio are dramatic. Comparing Figs. 4b and 5c, there is a clear tail in Fig. 4b on the right side of the 66-nm peak; this tail is due to a little misalignment of the interference optics.

Examples

Measurements and evaluations for the Latexmix Duke3060A/Duke3100A are shown in Figs. 6, 7, and 8. The results are summarized in Table 1. Measurements with interference optics (Fig. 6) yield the correct values of diameters and the mass ratio. Measurements with absorption optics at a wavelength of $\lambda_0=546$ nm (Fig. 7) exhibit the correct value of the ratio only if the Mie correction is applied; otherwise, the difference is substantial. For the wavelength of 263 nm, not only scattering but also absorption of the polystyrene

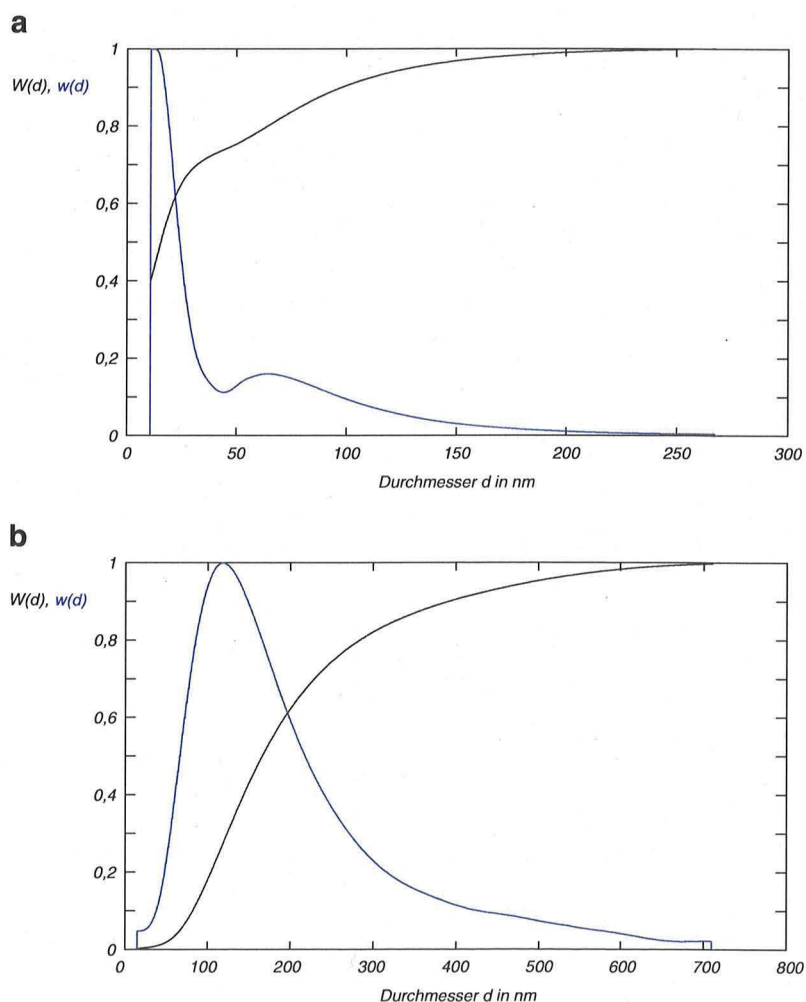
latexes has to be taken into account [21, 22]. Correct values of the mass ratio will be obtained applying Mie scattering and Mie absorption (Fig. 8 and Table 1).

Measurements and evaluations with absorption optics with respect to the blue pigment are shown in Fig. 9. The evaluations are done without imaginary part of the refractive index ($k_1=0$) and with imaginary part of the refractive index ($k_1=0.153$). It has been demonstrated that the differences are fairly large.

Summary and conclusion

It has been demonstrated that it is absolutely necessary to consider the Mie effect for the determination of the size distribution using absorption optics in the AUC OPTIMA XL-I. For particles which do not absorb but scatter, such as synthetic polymers and many inorganic substances at wavelengths in the visible region, it would be easy to

Fig. 9 OPTIMA XL, absorption optics: size distribution of a blue pigment in water. $C=0.612$ g/L, $\rho=1.39$ g/cm³, $\rho_0=0.997$ g/cm³, $n_0=1.333$, $n_1=1.30$, $\lambda_0=546$ nm, $N=0-40,000$ min⁻¹ (exponential increase); **a** $k_1=0$, **b** $k_1=0.153$ (absorption)



perform the Mie correction as the determination of the parameters (i.e., the refractive index of the particle) could be done using Eq. 18. For absorbing particles, one has to investigate whether absorption dominates the attenuation of the light beam. In this situation, the imaginary part of the refractive index could be determined using spectrometric measurements and Eq. 8. Otherwise, one has to perform spectrometric and light scattering measurements and then calculate k_1 using Eqs. 7, 8, 9, and 10.

The available programs for the evaluation of absorption measurements with the OPTIMA XL-I do not include the Mie effect since they were developed for the evaluation of polymer solutions where Mie scattering is not significant. However, for the analysis of nanoparticles using absorption optics, the Mie correction is mandatory due to their significant light scattering.

Acknowledgments We gratefully acknowledge the formulation of pigments by Dr. Theo Smit and excellent laboratory support from Manfred Stadler.

References

- Cölfen H (2005) In: Scott DJ, Harding SE, Rowe AJ (eds) Analytical ultracentrifugation techniques and methods. The Royal Society of Chemistry, Cambridge, pp 501–583
- Mächtle W, Börger L (2006) Analytical ultracentrifugation of polymers and nanoparticles. Springer, Berlin
- Scholtan W, Lange H (1972) Kolloid Z Z Polym 250:782–796
- Mächtle W (1984) Makromol Chem 185:1025–1039
- Planken KL, Cölfen H (2010) Nanoscale 2:1849–1869
- Bohren CF, Huffman DR (2004) Absorption and scattering of light by small particles. Wiley, New York
- Cölfen H, Harding SE (1995) Prog Colloid Polym Sci 99:167–186
- Mie G (1908) Ann Phys 25:377–443
- Dezelic G, Kratochvil JP (1960) Kolloid Z 173:38–48
- Lechner MD (2005) J Serb Chem Soc 70:361–369
- Barber PW, Hill SC (1990) Light scattering by particles: computational methods. World Scientific, Singapore
- Kerker M (1969) The scattering of light and other electromagnetic radiation. Academic, New York
- Bodman O (1969) Makromol Chem 122:196
- Müller H (1997) *Polymere Stabilisatoren in der Emulsionspolymerisation*, Thesis, Potsdam
- Bondy RH, Boyer RF (eds) (1952) Styrene, its polymers, copolymers and derivatives. Reinhold, New York
- Brandrup J, Immergut EH, Grulke EA (eds) (1999) Polymer handbook, 4th edn. Wiley, New York
- Mittal V, Völkel A, Cölfen H (2010) Macromol Biosci 10:754–762
- Fujita H (1975) Foundations of ultracentrifugal analysis. Wiley, New York
- Gosting LJ (1952) J Am Chem Soc 74:1548–1552
- Lechner MD, Mächtle W (1999) Prog Colloid Polym Sci 113:37–43
- Gantchev B, Mihailov B (1998) Polym Bull 41:207–213
- Holt Sackett P, Hannah RW, Slavin W (1978) Chromatographia 11:634–639